

## NANOCLUSTER FORMATION IN ELECTRON-IRRADIATED LITHIUM OXIDE

G. Krexner<sup>1</sup>, M. Prem<sup>2</sup>, F. Beuneu<sup>3</sup>, P. Vajda<sup>3</sup><sup>1</sup> Institute of Experimental Physics, University of Vienna, Boltzmanngasse 5, A-1090 Vienna, Austria<sup>2</sup> Laboratoire Léon Brillouin (CEA-CNRS), CEA- Saclay, 91191 Gif sur Yvette Cedex<sup>3</sup> Laboratoire des Solides Irradiés, Ecole Polytechnique (CEA-CNRS), F-91128 Palaiseau, France

Lithium oxide ( $\text{Li}_2\text{O}$ ) is a material of considerable interest both to applied and fundamental research: Being a superionic conductor it acts as a model substance for solid state batteries [1], due to its potential as a tritium breeder it is in discussion as a first-wall material in future fusion reactors [2], and its character as a highly ionic solid without  $d$  electrons renders it attractive for first principle calculations of electronic structures [3], among others.

Electron irradiation of  $\text{Li}_2\text{O}$  near ambient temperature induces the formation of metallic lithium precipitates (usually termed 'colloids') which were detected by conduction electron spin resonance,  $^7\text{Li}$ -nuclear magnetic resonance and differential scanning calorimetry [4-6]. Two types of lithium colloids were identified: Large precipitates with a typical size exceeding  $10\mu\text{m}$  (volume fraction  $\sim 2 \times 10^{-3}$ ) associated with molecular oxygen bubbles [7] and small lithium nanoclusters with a typical size of less than  $10\text{nm}$  and a volume fraction of about  $2 \times 10^{-5}$ . Attempts to characterize the structure and the arrangements of the lithium colloids with X-ray and electron scattering failed due to the low atomic number of lithium and its strongly ionic character. Therefore, a neutron scattering study was performed.

$\text{Li}_2\text{O}$  has a cubic antiferroite structure (space group  $\text{Fm}\bar{3}\text{m}$ ) with a lattice parameter of  $0.461\text{nm}$ . The sample used was a  $4 \times 7 \times 0.7\text{mm}$  platelet (weight  $\sim 40\text{mg}$ ) obtained from a float-zone grown single crystal. An unirradiated sample of similar dimensions served as a reference crystal. The sample was irradiated uniformly with  $1\text{MeV}$  electrons from a Van de Graaff accelerator at  $300\text{K}$  with a current of  $\sim 40\mu\text{A}/\text{cm}^2$  up to a dose of  $15\text{C}/\text{cm}^2$ . The neutron scattering experiments were performed on the triple-axis spectrometer G4.3 VALSE located at a cold neutron guide at the LLB. The wavelength used was  $0.292\text{nm}$ . A pyrolytic graphite analyser was set in the second order position leading to an improved resolution  $<0.01\text{\AA}^{-1}$  for radial scans. In addition, the discrimination of inelastic scattering contributions resulted in a favourably low background level.

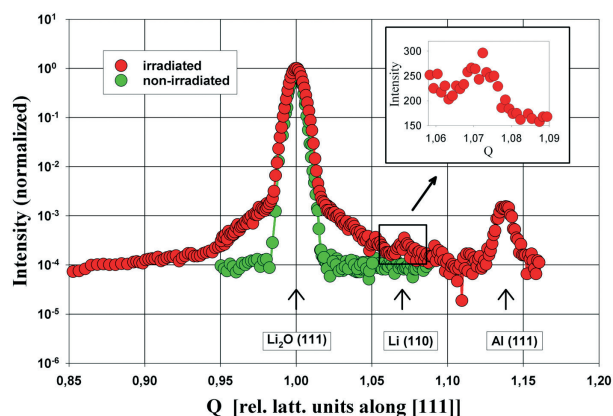


Figure 1. High-resolution radial scan through the (111) Bragg peak of the  $\text{Li}_2\text{O}$  matrix. The intensity is plotted on a logarithmic scale. The small peak at  $Q \sim 1.07$  (see inset) corresponds to the Li (110) reflection of the large lithium colloids. The intensity at  $Q \sim 1.14$  belongs to the aluminium (111) Debye-Scherrer line due to the sample wrapping. Distortion scattering around the (111) Bragg position of the matrix is clearly recognizable.

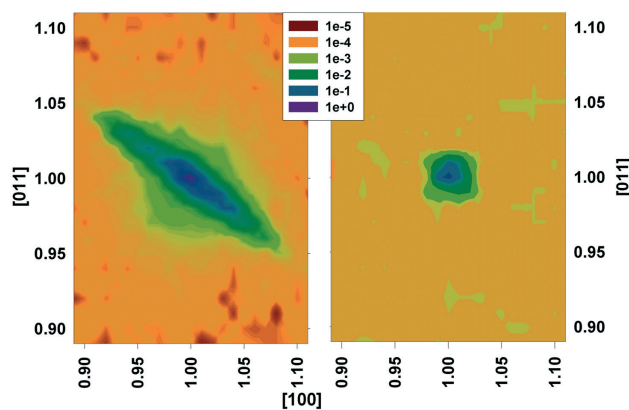


Figure 2. Diffuse scattering observed around the (111) Bragg peak of the  $\text{Li}_2\text{O}$  matrix in an irradiated (left) and an unirradiated (right) crystal. Results for the (200) and (220) peaks are similar.

Elastic diffuse scattering around the (111), (200) and (220) Bragg peaks was studied in a (110) scattering plane (Figs.1,2). In Fig. 3 the distortion scattering observed radially close to the (200) and (111) Bragg peaks is displayed, after background correction, in a doubly-logarithmic plot. The regions of Huang and asymptotic (Stokes-Wilson) scattering can be easily identified. The details of the intensity decrease that are observed beyond the

Huang region depend strongly on the type of defect giving rise to the scattering and may be different for the two sides of the Bragg peak as observed for the (111) peak in this study.

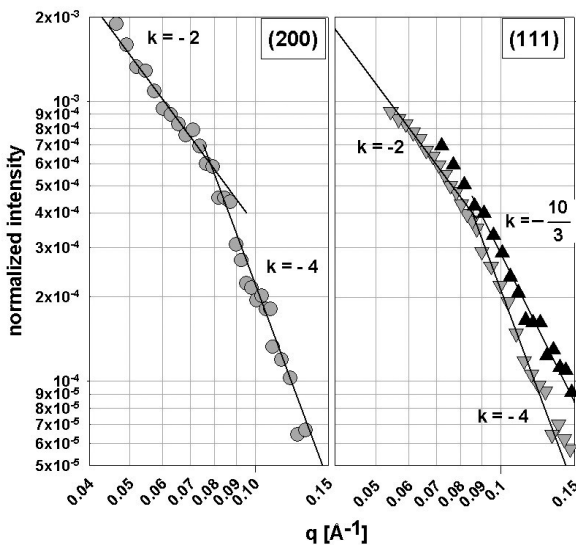


Figure 3. Distortion scattering close to the (200) and (111) Bragg peaks displayed on a doubly-logarithmic scale. For the (200) peak the symmetrized scattering distribution is shown. For the (111) peak the scattering at the low- $Q$  and the high- $Q$  side are plotted separately. The scattering first decreases as  $q^{-2}$  ('Huang scattering') followed by a  $q^{-4}$  or  $q^{-10/3}$  dependence ('Stokes-Wilson scattering'). The crossover permits to determine the approximate size of the defect (i.e. the small colloids in the present case) along a particular direction.

Combining the data from several peaks and the observed lattice parameter shift due to irradiation provides information on the concentration of the small colloids and the associated distortion field. Careful evaluation [8,9] yields typical diameters of the defect clusters of  $8 \times 8 \times 4$  nm along the crystallographic directions [011], [0-11] and [100], respectively. These values are in good accordance with small-angle scattering data of the same sample (not shown here) yielding an averaged Guinier radius of  $\sim 2.5$  nm corresponding to a mean geometrical diameter of about 6.5 nm and about 10 000 Li atoms in one cluster.

## References

- [1] N. Roux, C. Johnson, and K. Noda, *J. Nucl. Mater.* **191/194**, 15 (1992).
- [2] Y. Oishi *et al.*, *J. Nucl. Mater.* **87**, 341 (1979).
- [3] S. Albrecht, G. Onida, and L. Reining, *Phys. Rev. B* **55**, 10 278 (1997).
- [4] F. Beuneu, P. Vajda, *Phys. Rev. Lett.* **76**, 4544 (1996).
- [5] P. Vajda, F. Beuneu, *Phys.Rev.B* **53**, 5335 (1996).
- [6] F. Beuneu, P. Vajda, G. Jaskierowicz, M. Lafleuruelle *Phys. Rev. B* **55**, 11263 (1997).
- [7] F. Beuneu, P. Vajda, O. J. Zogal, *Phys.Rev.Lett.* **83**, 761 (1999).
- [8] P. Vajda, F. Beuneu, G. Krexner, M. Prem, O. Blaschko, and C. Maier, *Nucl. Instr. Meth. B* **166-167**, 275 (2000).
- [9] G. Krexner, M. Prem, F. Beuneu, and P. Vajda, *Phys.Rev. Lett.* **91**, 135502 (2003).
- [10] M. Prem, G. Krexner, F. Beuneu, and P. Vajda, *Physica B: Cond.Matter* **350**, Suppl. 1, p. E999 (2004).

The distortion scattering due to the small colloids was also investigated as a function of temperature and was found to remain unchanged on cooling from ambient temperature down to 30 K [10]. This means that, contrary to the large colloids [7], the small Li precipitates cannot be associated with oxygen bubbles. The volume change of oxygen upon freezing (about three orders of magnitude) would lead to a significant relaxation of the lattice strain around the defect clusters. This change, in turn, would lead to a concomitant decrease of the intensity of the observed distortion scattering which, however, was not found in the experiment.

For the large colloids, measurements of several well defined Bragg peaks – cf. the (110) peak in Fig.1 – confirm their composition to be elemental *bcc* lithium. Their orientation relations with respect to the  $\text{Li}_2\text{O}$  matrix is shown in Fig.4. It is defined by  $[110]_{\text{Li}} \parallel [211]_{\text{Li}_2\text{O}} \pm 4.4^\circ$  (two variants), and  $[001]_{\text{Li}} \parallel [011]_{\text{Li}_2\text{O}} \pm 4.4^\circ$  (two variants). The deviation of slightly more than  $4^\circ$  is due to the lattice misfit between matrix and precipitates. Perpendicularly to the plane shown in Fig. 4 the orientation relation is  $[110]_{\text{Li}} \parallel [111]_{\text{Li}_2\text{O}}$ .

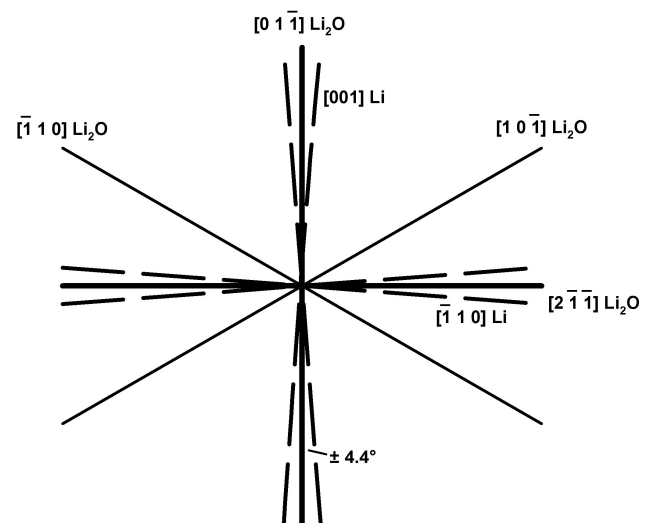


Figure 4. Orientation relation between the  $\text{Li}_2\text{O}$  matrix and the large lithium colloids.